SUPPLEMENTAL INFORMATION

Supplemental Figures

Figure S1.

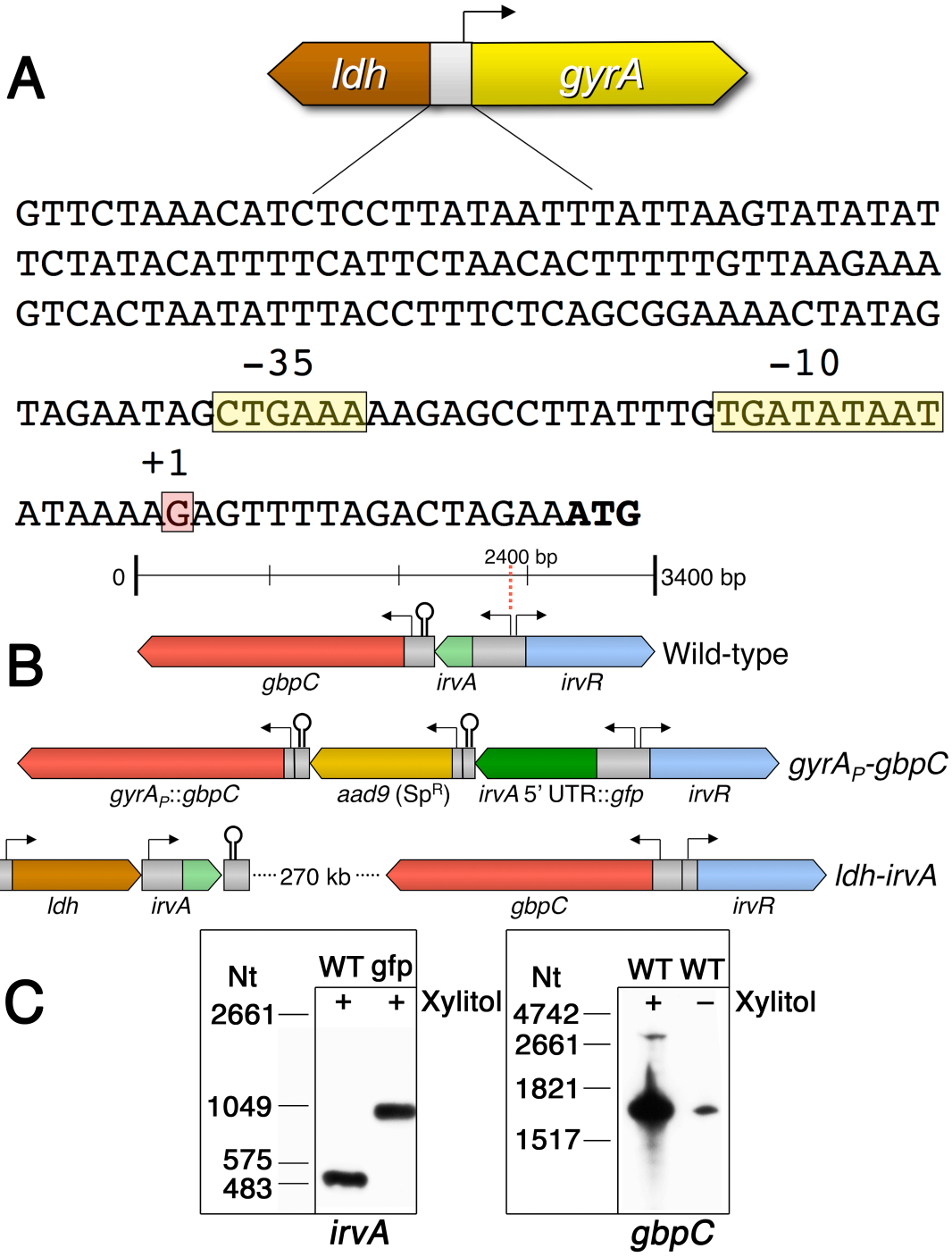

Fig. S1. Chromosomal maps and transcriptional analyses of *irvA* and *gbpC* genetic constructs. Related to Figures 1, 2, and 4. A) 5' RACE PCR was used to identify the transcription start site of the *gyrA* gene. The organization of the *gyrA* locus and the sequence of the upstream intergenic region are shown. Promoter elements are highlighted in yellow, the *gyrA* transcription start site is shown in red, and the annotated *gyrA* initiation codon is shown in bold print. A portion of the

intergenic region up to the -1 site was used to drive the expression of *gbpC* in the $gyrA_P$–*gbpC* fusion strain. B) The genomic organization of the *irvA* locus is shown for the wild-type, $gyrA_P$-*gbpC*, and *ldh*-*irvA* strains. Coding regions are shown in various colors, while non-coding regions are shown in grey. As shown in the scalebar, a read-through transcript from *irvA* would be predicted to be approximately 2.4 kb. C) Both the *irvA* wild-type (WT) and 5' UTR-*gfp* fusion (gfp) strains as well as the wild-type *gbpC* (WT) were assayed via northern blot to confirm transcript sizes and test for the presence of additional read-through transcripts. The *irvA* samples were derived from cultures grown in the presence of xylitol stress, while the *gbpC* samples were derived from cultures grown both in the presence and absence of xylitol. The *irvA* northern blot was probed in a single blot using a mixture of *irvA* CDS and *gfp* ORF probes that were previously determined to lack cross-hybridization. No read-through transcripts were detectable using the *irvA* probes, whereas a very minor read-through transcript was detectable using the *gbpC* probe. This corresponds to a previously reported transcript created from read-though downstream of *gbpC* (Biswas et al., 2007).

Figure S2.

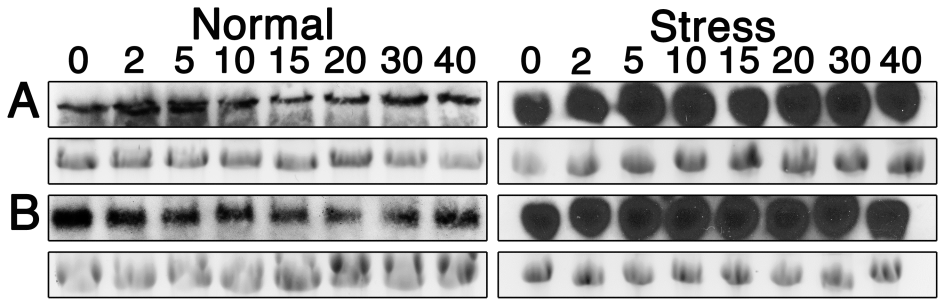

Fig. S2. mRNA stability assay of *irvA* 5' UTR-*gfp* ORF fusion. Related to Figure 2. The numbers above the figures indicate the time (min.) after the addition of rifampicin for mRNA stability assays. For each figure, the top panels show target mRNA northern blots and bottom panels are 16S rRNA loading controls. The mRNA turnover rate of the *irvA* 5' UTR-*gfp* ORF fusion strain was assayed in normal and stress growth conditions. The northern blot probes hybridize within the *gfp* ORF. mRNA stability was measured both in a A) wild-type *gbpC* background and B) *gbpC* 5' UTR truncated background.

Figure S3.

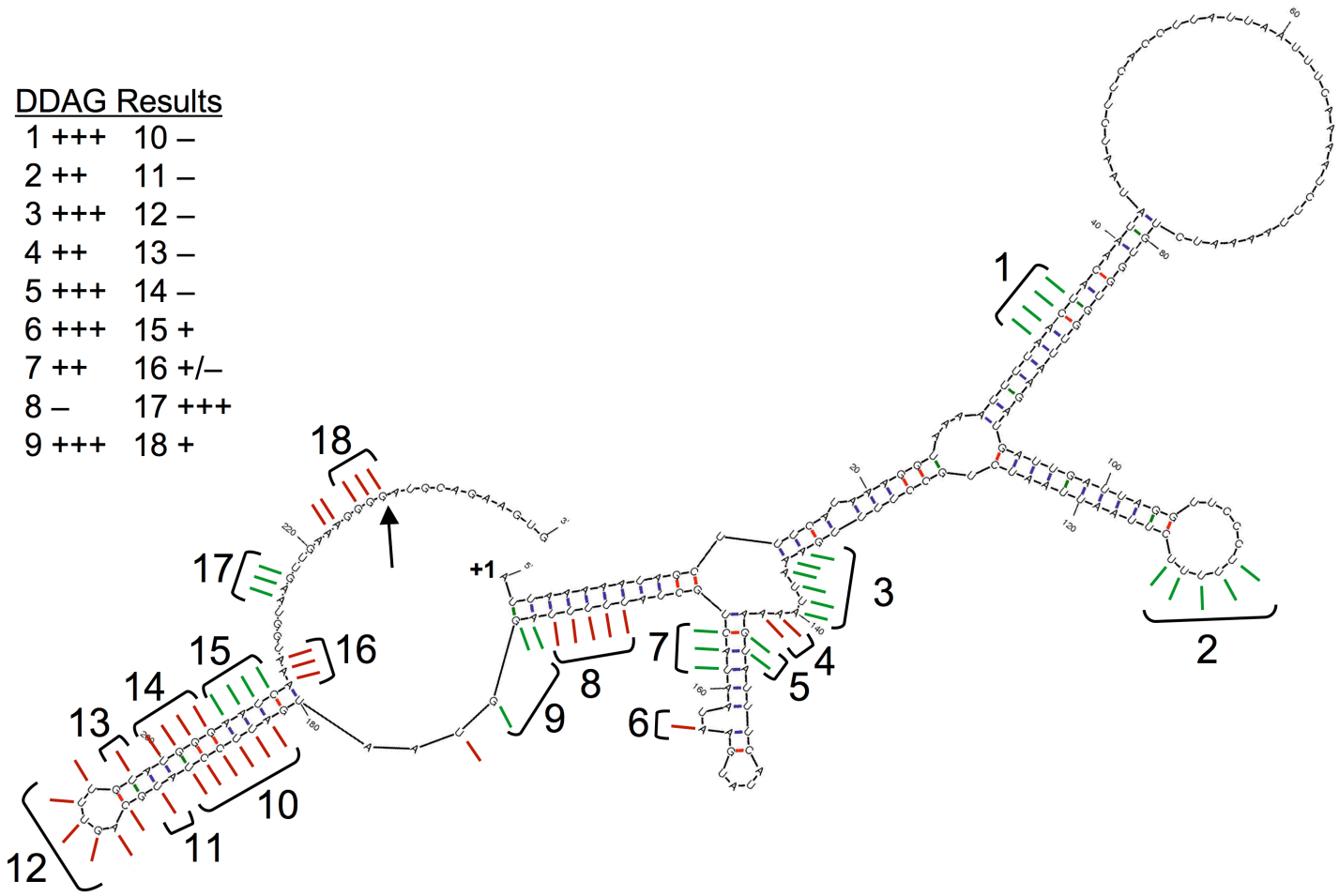

Fig. S3. High throughput mutagenesis of WT *irvA* to determine critical residues for DDAG. Related to Figures 4 and 5. A modified error-prone PCR protocol created a large pool of *irvA* mutant templates with >20 mutations per template on average. These were transformed into *S. mutans* to create a pool of 80,000 *irvA* mutant strains. The pool was mixed, sonicated, and separated in a large DDAG assay. Non-aggregators were sequenced using Illumina. Data were aligned and the mutagenesis frequency was calculated for each base. Significantly overrepresented bases are marked in red. No significant bases were detected in the *irvA* ORF, so only the 5' UTR is shown. Several predicted critical and noncritical bases were mutagenized and tested for their role in DDAG. Mutation sites are marked with brackets. Bases marked in green were determined to be statistically insignificant for DDAG and were tested as negative controls. An arrow marks the crosslink site identified in the RACE walk experiment. The *irvA* +1 site is indicated. The DDAG scale is as follows: +++ (Strong DDAG evident in <2 min), ++ (Strong DDAG evident in ≤5 min), + (Moderate DDAG evident in 5 – 10 min), +/– (Weak DDAG evident in ≥ 10 min), and – (No DDAG evident). Bases located in sections 11 – 14 were further tested for their role in mediating seed pairing with *gbpC* in Figure 5.

Figure S4.

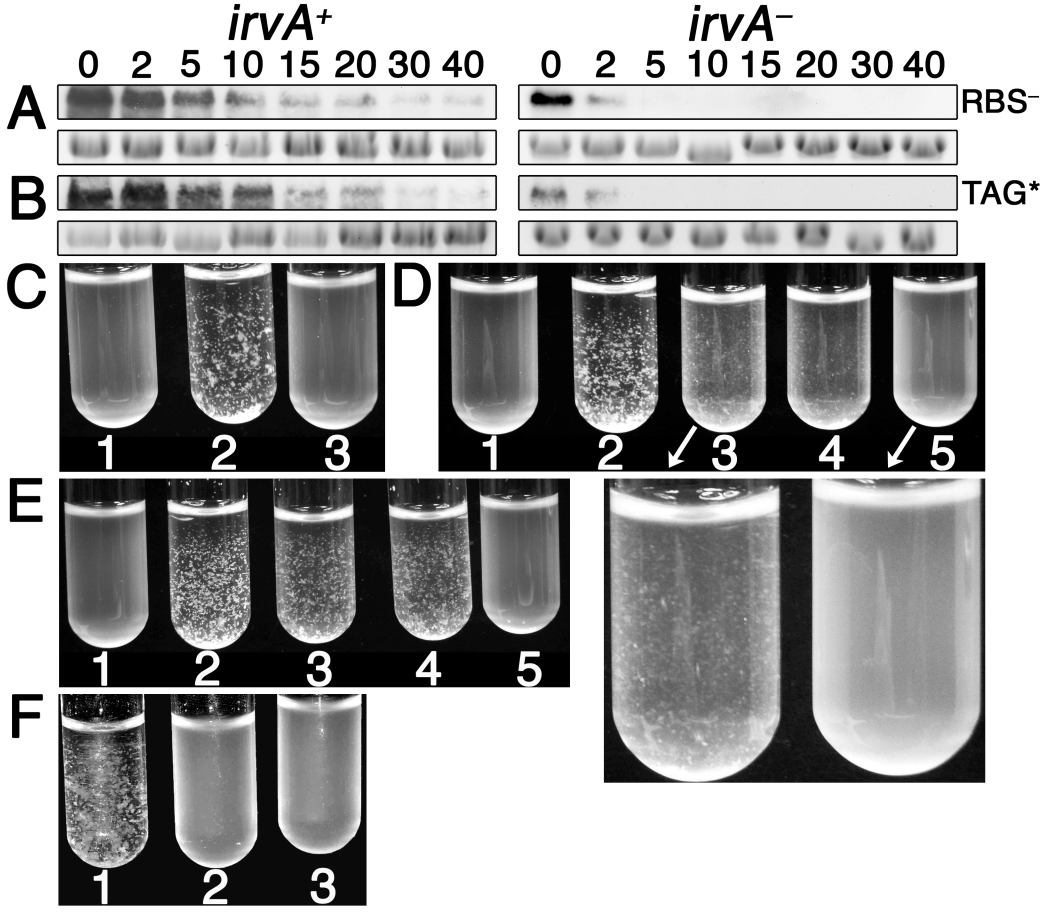

Fig. S4. GbpC production is primarily inhibited by RNase J2 in the absence of stress. Related to Figure 6. In panels A and B, the numbers above the figures signify the time after rifampicin addition for mRNA stability assays of *gbpC* mRNA. The bottom panels are 16S rRNA loading controls. The mRNA stability assays were performed using *gbpC* containing the following mutations: A) point mutations in the Shine-Dalgarno sequence (RBS^{-}) and B) premature stop codon after the initiation codon (TAG*). Cultures in C – F were grown to mid-log phase. C) Strains from left to right: 1. wild-type; 2. wild-type + xylitol stress; and 3. RNase J1 mutant D) Strains from left to right: 1. wild-type; 2. wild-type + xylitol stress; 3. RNase Y mutant; 4. RNase Y/*irvA* double mutant; and 5. RNase Y mutant + *trans*-expressed *rny* (To better illustrate the weak DDAG phenotype, images of the Δ*rny* and complemented cultures were magnified.) E) Strains from left to right: 1. wild-type; 2. wild-type + xylitol stress; 3. RNase J2 mutant; 4. RNase J2/*irvA* double mutant; and 5. RNase J2 mutant + *trans*-expressed *rnjB*. F) Strains from left to right: 1. RNase J2 mutant; 2. RNase J2/GbpC double mutant; and 3. wild-type

Figure S5.

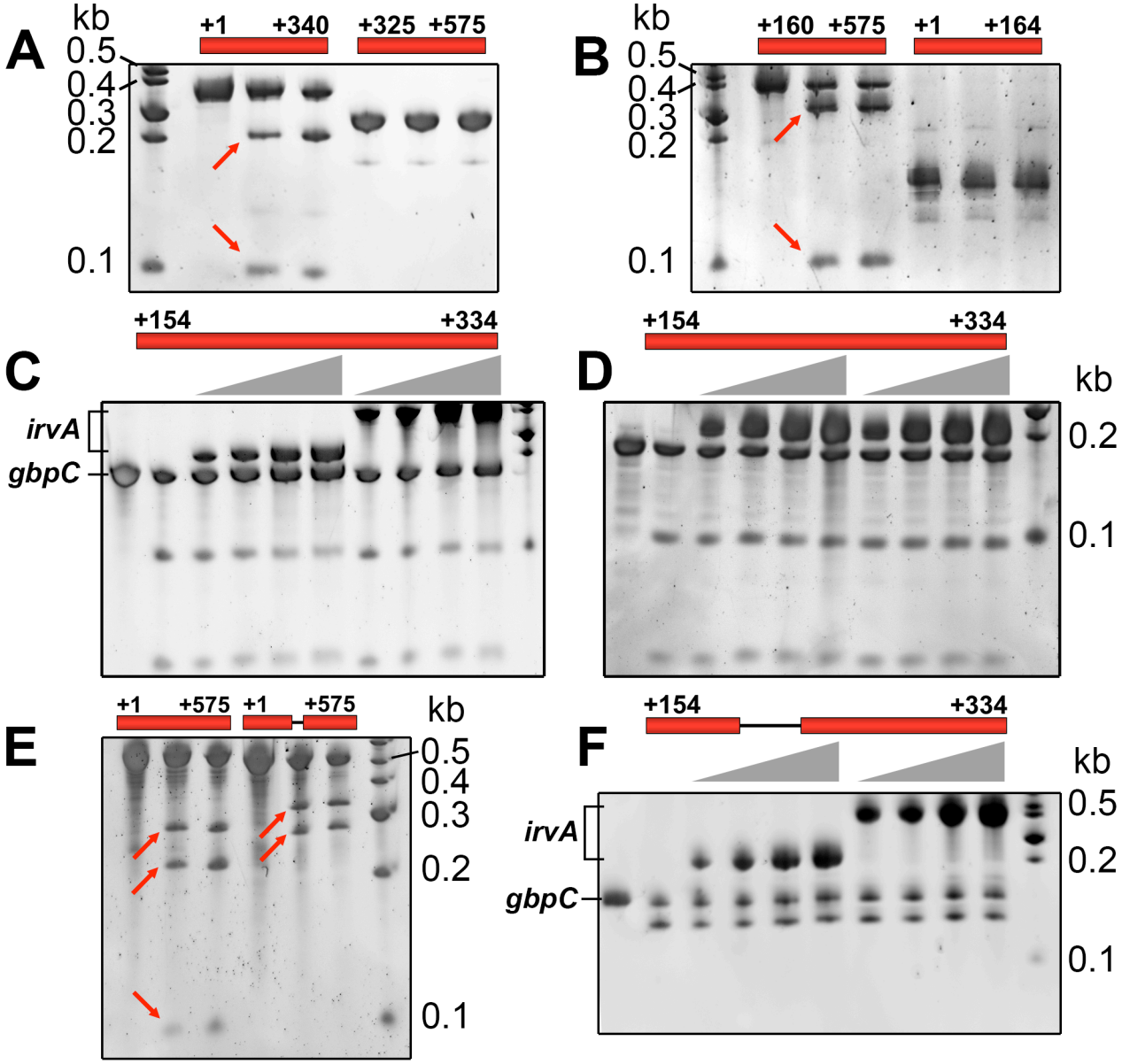

Fig. S5. Determination of the RNase J2 cleavage site region in *gbpC* mRNA. Related to Figure 6. Maps above each figure indicate the portion of *gbpC* that was assayed for *in vitro* cleavage by RNase J2. A) Two fragments of *gbpC* that together span the entire *gbpC* RACE walk interaction domain were digested with RNase J2. Each fragment was assayed in three separate reactions shown from left to right: untreated RNA, 15 minute digest with RNase J2, and 30 minute digest with RNase J2. Two stable intermediate cleavage products are shown. A third ~30 nt band is present, but only resolvable using a high percentage gel (data not shown) indicating that the mRNA was cut twice by RNase J2. B) A similar reaction was performed as in S6A, but different fragments within the *gbpC* RACE walk interaction domain were digested. A third ~50 nt cleavage product was also detectable using a high percentage gel (data not shown). C) The indicated region of *gbpC* was digested with RNase J2 in the absence and presence of *irvA*. The lanes from left to right are: untreated *gbpC*, digested *gbpC*, four reactions of *gbpC* digested in the presence of increasing amounts of wild-type *irvA* UTR, and four reactions of *gbpC* digested in the presence of increasing amounts of the full-length wild-type *irvA*. Both species of these *irvA* molecules yielded a discernable concentration-dependent inhibitory effect upon RNase J2 cleavage of *gbpC*. A third ~25 nt band is present, but only resolvable

using a high percentage gel (data not shown). D) A similar experiment was performed as in S6C, except increasing amounts of either interaction-deficient mutant *irvA* UTR (first set of four reactions) or *irvA* ORF (second set of four reactions) were included in the *gbpC* digestion. The presence of these *irvA* fragments had no observable impact upon the efficiency of *gbpC* cleavage. E) Two fragments of *gbpC* that each spans the entire *gbpC* RACE walk interaction domain were digested with RNase J2. Each fragment was assayed in three separate reactions shown from left to right: untreated RNA, 15 minute digest with RNase J2, and 30 minute digest with RNase J2. The first set of digests was performed on wild-type *gbpC* mRNA, while the second set contained *gbpC* lacking the *irvA*-controlled RNase J2 cleavage site. Arrows indicate the expected cleavage products. F) The wild-type *irvA* UTR and full-length mRNA were both tested for their ability to inhibit RNase J2 cleavage of *gbpC* lacking the *irvA*-controlled RNase J2 cleavage site. Neither of the two *irvA* molecules yielded obvious inhibition of RNase J2 cleavage towards the second cleavage site. The expected ~130 nt weight cleavage product was visible, whereas the second ~25 nt band was only resolvable using a high percentage gel (data not shown).

Figure S6.

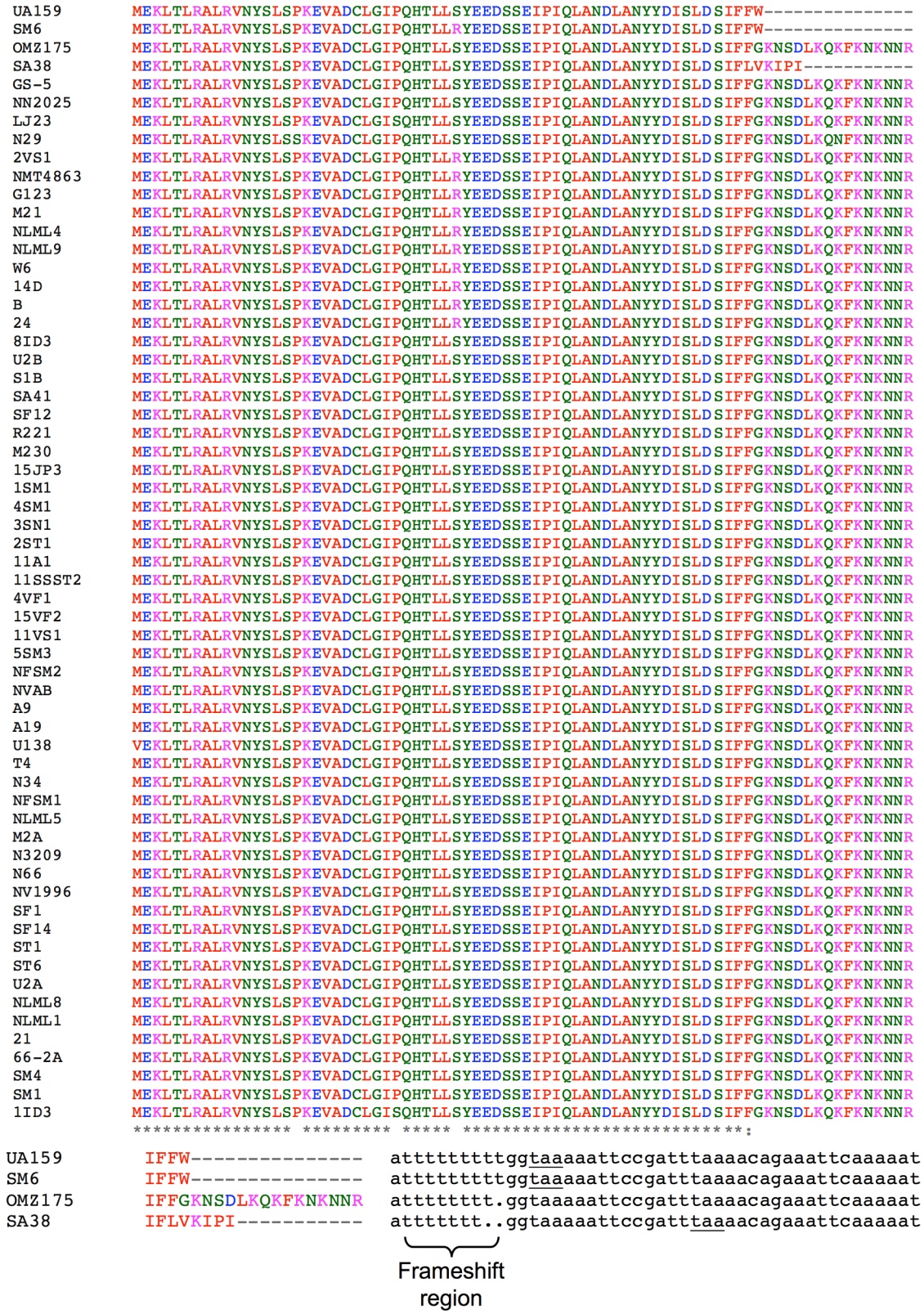
UA159 MEKLTLRALRVNYSLSPKEVADCLGIPQHTLLSYEEDSSEIPIQLANDLANYYDISLDSIFFW----------
SM6 MEKLTLRALRVNYSLSPKEVADCLGIPQHTLLRYEEDSSEIPIQLANDLANYYDISLDSIFFW----------
OMZ175 MEKLTLRALRVNYSLSPKEVADCLGIPQHTLLSYEEDSSEIPIQLANDLANYYDISLDSIFFGKNSDLKQKFKNKNNR
SA38 MEKLTLRALRVNYSLSPKEVADCLGIPQHTLLSYEEDSSEIPIQLANDLANYYDISLDSIFLVKIPI----------
GS-5 MEKLTLRALRVNYSLSPKEVADCLGIPQHTLLSYEEDSSEIPIQLANDLANYYDISLDSIFFGKNSDLKQKFKNKNNR
NN2025 MEKLTLRALRVNYSLSPKEVADCLGIPQHTLLSYEEDSSEIPIQLANDLANYYDISLDSIFFGKNSDLKQKFKNKNNR
LJ23 MEKLTLRALRVNYSLSPKEVADCLGISQHTLLSYEEDSSEIPIQLANDLANYYDISLDSIFFGKNSDLKQKFKNKNNR
N29 MEKLTLRALRVNYSLSSKEVADCLGIPQHTLLSYEEDSSEIPIQLANDLANYYDISLDSIFFGKNSDLKQNFKNKNNR
2VS1 MEKLTLRALRVNYSLSPKEVADCLGIPQHTLLRYEEDSSEIPIQLANDLANYYDISLDSIFFGKNSDLKQKFKNKNNR
NMT4863 MEKLTLRALRVNYSLSPKEVADCLGIPQHTLLRYEEDSSEIPIQLANDLANYYDISLDSIFFGKNSDLKQKFKNKNNR
G123 MEKLTLRALRVNYSLSPKEVADCLGIPQHTLLRYEEDSSEIPIQLANDLANYYDISLDSIFFGKNSDLKQKFKNKNNR
M21 MEKLTLRALRVNYSLSPKEVADCLGIPQHTLLRYEEDSSEIPIQLANDLANYYDISLDSIFFGKNSDLKQKFKNKNNR
NLML4 MEKLTLRALRVNYSLSPKEVADCLGIPQHTLLRYEEDSSEIPIQLANDLANYYDISLDSIFFGKNSDLKQKFKNKNNR
NLML9 MEKLTLRALRVNYSLSPKEVADCLGIPQHTLLRYEEDSSEIPIQLANDLANYYDISLDSIFFGKNSDLKQKFKNKNNR
W6 MEKLTLRALRVNYSLSPKEVADCLGIPQHTLLRYEEDSSEIPIQLANDLANYYDISLDSIFFGKNSDLKQKFKNKNNR
14D MEKLTLRALRVNYSLSPKEVADCLGIPQHTLLRYEEDSSEIPIQLANDLANYYDISLDSIFFGKNSDLKQKFKNKNNR
B MEKLTLRALRVNYSLSPKEVADCLGIPQHTLLRYEEDSSEIPIQLANDLANYYDISLDSIFFGKNSDLKQKFKNKNNR
24 MEKLTLRALRVNYSLSPKEVADCLGIPQHTLLRYEEDSSEIPIQLANDLANYYDISLDSIFFGKNSDLKQKFKNKNNR
8ID3 MEKLTLRALRVNYSLSPKEVADCLGIPQHTLLSYEEDSSEIPIQLANDLANYYDISLDSIFFGKNSDLKQKFKNKNNR
U2B MEKLTLRALRVNYSLSPKEVADCLGIPQHTLLSYEEDSSEIPIQLANDLANYYDISLDSIFFGKNSDLKQKFKNKNNR
S1B MEKLTLRALRVNYSLSPKEVADCLGIPQHTLLSYEEDSSEIPIQLANDLANYYDISLDSIFFGKNSDLKQKFKNKNNR
SA41 MEKLTLRALRVNYSLSPKEVADCLGIPQHTLLSYEEDSSEIPIQLANDLANYYDISLDSIFFGKNSDLKQKFKNKNNR
SF12 MEKLTLRALRVNYSLSPKEVADCLGIPQHTLLSYEEDSSEIPIQLANDLANYYDISLDSIFFGKNSDLKQKFKNKNNR
R221 MEKLTLRALRVNYSLSPKEVADCLGIPQHTLLSYEEDSSEIPIQLANDLANYYDISLDSIFFGKNSDLKQKFKNKNNR
M230 MEKLTLRALRVNYSLSPKEVADCLGIPQHTLLSYEEDSSEIPIQLANDLANYYDISLDSIFFGKNSDLKQKFKNKNNR
15JP3 MEKLTLRALRVNYSLSPKEVADCLGIPQHTLLSYEEDSSEIPIQLANDLANYYDISLDSIFFGKNSDLKQKFKNKNNR
1SM1 MEKLTLRALRVNYSLSPKEVADCLGIPQHTLLSYEEDSSEIPIQLANDLANYYDISLDSIFFGKNSDLKQKFKNKNNR
4SM1 MEKLTLRALRVNYSLSPKEVADCLGIPQHTLLSYEEDSSEIPIQLANDLANYYDISLDSIFFGKNSDLKQKFKNKNNR
3SN1 MEKLTLRALRVNYSLSPKEVADCLGIPQHTLLSYEEDSSEIPIQLANDLANYYDISLDSIFFGKNSDLKQKFKNKNNR
2ST1 MEKLTLRALRVNYSLSPKEVADCLGIPQHTLLSYEEDSSEIPIQLANDLANYYDISLDSIFFGKNSDLKQKFKNKNNR
11A1 MEKLTLRALRVNYSLSPKEVADCLGIPQHTLLSYEEDSSEIPIQLANDLANYYDISLDSIFFGKNSDLKQKFKNKNNR
11SSST2 MEKLTLRALRVNYSLSPKEVADCLGIPQHTLLSYEEDSSEIPIQLANDLANYYDISLDSIFFGKNSDLKQKFKNKNNR
4VF1 MEKLTLRALRVNYSLSPKEVADCLGIPQHTLLSYEEDSSEIPIQLANDLANYYDISLDSIFFGKNSDLKQKFKNKNNR
15VF2 MEKLTLRALRVNYSLSPKEVADCLGIPQHTLLSYEEDSSEIPIQLANDLANYYDISLDSIFFGKNSDLKQKFKNKNNR
11VS1 MEKLTLRALRVNYSLSPKEVADCLGIPQHTLLSYEEDSSEIPIQLANDLANYYDISLDSIFFGKNSDLKQKFKNKNNR
5SM3 MEKLTLRALRVNYSLSPKEVADCLGIPQHTLLSYEEDSSEIPIQLANDLANYYDISLDSIFFGKNSDLKQKFKNKNNR
NFSM2 MEKLTLRALRVNYSLSPKEVADCLGIPQHTLLSYEEDSSEIPIQLANDLANYYDISLDSIFFGKNSDLKQKFKNKNNR
NVAB MEKLTLRALRVNYSLSPKEVADCLGIPQHTLLSYEEDSSEIPIQLANDLANYYDISLDSIFFGKNSDLKQKFKNKNNR
A9 MEKLTLRALRVNYSLSPKEVADCLGIPQHTLLSYEEDSSEIPIQLANDLANYYDISLDSIFFGKNSDLKQKFKNKNNR
A19 MEKLTLRALRVNYSLSPKEVADCLGIPQHTLLSYEEDSSEIPIQLANDLANYYDISLDSIFFGKNSDLKQKFKNKNNR
U138 VEKLTLRALRVNYSLSPKEVADCLGIPQHTLLSYEEDSSEIPIQLANDLANYYDISLDSIFFGKNSDLKQKFKNKNNR
T4 MEKLTLRALRVNYSLSPKEVADCLGIPQHTLLSYEEDSSEIPIQLANDLANYYDISLDSIFFGKNSDLKQKFKNKNNR
N34 MEKLTLRALRVNYSLSPKEVADCLGIPQHTLLSYEEDSSEIPIQLANDLANYYDISLDSIFFGKNSDLKQKFKNKNNR
NFSM1 MEKLTLRALRVNYSLSPKEVADCLGIPQHTLLSYEEDSSEIPIQLANDLANYYDISLDSIFFGKNSDLKQKFKNKNNR
NLML5 MEKLTLRALRVNYSLSPKEVADCLGIPQHTLLSYEEDSSEIPIQLANDLANYYDISLDSIFFGKNSDLKQKFKNKNNR
M2A MEKLTLRALRVNYSLSPKEVADCLGIPQHTLLSYEEDSSEIPIQLANDLANYYDISLDSIFFGKNSDLKQKFKNKNNR
N3209 MEKLTLRALRVNYSLSPKEVADCLGIPQHTLLSYEEDSSEIPIQLANDLANYYDISLDSIFFGKNSDLKQKFKNKNNR
N66 MEKLTLRALRVNYSLSPKEVADCLGIPQHTLLSYEEDSSEIPIQLANDLANYYDISLDSIFFGKNSDLKQKFKNKNNR
NV1996 MEKLTLRALRVNYSLSPKEVADCLGIPQHTLLSYEEDSSEIPIQLANDLANYYDISLDSIFFGKNSDLKQKFKNKNNR
SF1 MEKLTLRALRVNYSLSPKEVADCLGIPQHTLLSYEEDSSEIPIQLANDLANYYDISLDSIFFGKNSDLKQKFKNKNNR
SF14 MEKLTLRALRVNYSLSPKEVADCLGIPQHTLLSYEEDSSEIPIQLANDLANYYDISLDSIFFGKNSDLKQKFKNKNNR
ST1 MEKLTLRALRVNYSLSPKEVADCLGIPQHTLLSYEEDSSEIPIQLANDLANYYDISLDSIFFGKNSDLKQKFKNKNNR
ST6 MEKLTLRALRVNYSLSPKEVADCLGIPQHTLLSYEEDSSEIPIQLANDLANYYDISLDSIFFGKNSDLKQKFKNKNNR
U2A MEKLTLRALRVNYSLSPKEVADCLGIPQHTLLSYEEDSSEIPIQLANDLANYYDISLDSIFFGKNSDLKQKFKNKNNR
NLML8 MEKLTLRALRVNYSLSPKEVADCLGIPQHTLLSYEEDSSEIPIQLANDLANYYDISLDSIFFGKNSDLKQKFKNKNNR
NLML1 MEKLTLRALRVNYSLSPKEVADCLGIPQHTLLSYEEDSSEIPIQLANDLANYYDISLDSIFFGKNSDLKQKFKNKNNR
21 MEKLTLRALRVNYSLSPKEVADCLGIPQHTLLSYEEDSSEIPIQLANDLANYYDISLDSIFFGKNSDLKQKFKNKNNR
66-2A MEKLTLRALRVNYSLSPKEVADCLGIPQHTLLSYEEDSSEIPIQLANDLANYYDISLDSIFFGKNSDLKQKFKNKNNR
SM4 MEKLTLRALRVNYSLSPKEVADCLGIPQHTLLSYEEDSSEIPIQLANDLANYYDISLDSIFFGKNSDLKQKFKNKNNR
SM1 MEKLTLRALRVNYSLSPKEVADCLGIPQHTLLSYEEDSSEIPIQLANDLANYYDISLDSIFFGKNSDLKQKFKNKNNR
1ID3 MEKLTLRALRVNYSLSPKEVADCLGISQHTLLSYEEDSSEIPIQLANDLANYYDISLDSIFFGKNSDLKQKFKNKNNR
UA159 IFFW---------- atttttttttggtaaaaattccgatttaaaacagaaattcaaaaat
SM6 IFFW---------- atttttttttggtaaaaattccgatttaaaacagaaattcaaaaat
OMZ175 IFFGKNSDLKQKFKNKNNR atttttttt.ggtaaaaattccgatttaaaacagaaattcaaaaat
SA38 IFLVKIPI---------- atttttttt..ggtaaaaattccgatttaaaacagaaattcaaaaat
Frameshift region

Fig. S6. Analysis of IrvA proteins from 57 strains of *S. mutans*. Related to Figure 7. CLUSTAL Ω (http://www.ebi.ac.uk/Tools/msa/clustalo/) was used to align the *irvA* ORFs from 57 sequenced isolates of *S. mutans*. The genome reference strain UA159 is listed first. The source of C-terminal IrvA truncations in the wild-type strains UA159, SM6, and SA38 is due to the presence of frameshift mutations within a long stretch of thymidines near the 3' of *irvA* (shown at the bottom of the figure). Both UA159 and SM6 have an insertion of an additional thymidine, whereas strain SA38 has a single thymidine deletion. Strain OMZ175 contains the full-length *irvA* ORF found in the vast majority of *S. mutans* isolates.

Supplemental Tables

Table S1.

Strain/plasmid	Characteristics	Figures	Reference/Source
E. coli			
JM109	e14$^-$(McrA$^-$) *recA1 endA1gyrA96 thi-1 hsdR17*(r_K^- m_K^+) *supE44 relA1* Δ(*lac-proAB*) [F' *traD36 proAB lacI$_q$Z* Δ*M15*]		Cloning strain
S. mutans			
UA159	*S. mutans* genome reference strain	Fig. 1, 2, 4, 6, 7, S1, S4	(Ajdic et al., 2002)
IFD	UA159::IFDC2, Em^r, *p*-Cl-Phe^s		This work
RKO	UA159 Δ*irvR*, Em^s, *p*-Cl-Phe^r	Fig. 1	This work
ALDGFP	UA159 Δ*irvA* ORF, *irvA* 5' UTR::*gfp*, Em^s, *p*-Cl-Phe^r	Fig. 1	This work
AKO	UA159 Δ*irvA*, Em^s, *p*-Cl-Phe^r	Fig. 1	This work
AKO-IFD2	UA159 Δ*irvA*, Em^r, *p*-Cl-Phe^s		This work
CKO-IFD2	UA159 Δ*gbpC*, Em^r, *p*-Cl-Phe^s		This work
CKO	UA159 Δ*gbpC*, Em^s, *p*-Cl-Phe^r	Fig. 1	This work
COMA	UA159::pDL278A, Δ*irvA*, Sp^r, Em^s, *p*-Cl-Phe^r	Fig. 1	This work
AORFR	UA159 Δ*irvA* ORF, Δ*irvR*, Em^s, *p*-Cl-Phe^r	Fig.1	This work
AKOR	UA159 Δ*irvA*, Δ*irvR*, Em^s, *p*-Cl-Phe^r	Fig. 1	This work
COMAR	UA159::pDL278A, Δ*irvA*, Δ*irvR*, Km^r, Sp^r	Fig. 1	This work
GAGBPC	UA159 *gyrA$_P$*::*gbpC*, Sp^r	Fig. 2	This work
CALD	UA159 *gyrA$_P$-gbpC*, *irvA* 5' UTR::*gfp*, Sp^r	Fig. 2, 4	This work
ASTD3	UA159 *gyrA$_P$-gbpC*, *irvA* 5' UTR Δ$^+$180-$^+$210::*gfp*, Sp^r	Fig. 4	This work
CLD	UA159 *gyrA$_P$-gbpC*, *irvA$_P$*::*gfp*, Sp^r	Fig. 2, 4, S1	This work
ALD	UA159 *gyrA$_P$-gbpC*, Δ*gbpC* 5' UTR, *irvA* 5' UTR::*gfp*, Sp^r	Fig. 2, 4, S1	This work
CALDKO	UA159 *gyrA$_P$-gbpC*, Δ*gbpC* 5' UTR, *irvA$_P$*::*gfp*, Sp^r	Fig. 2	This work

AFLA	UA159 *irvA*::FLAG, Em^s, *p*-Cl-Phe^r	Fig. 7	This work
AFLAR	UA159 Δ*irvR*, *irvA*::FLAG, Em^s, *p*-Cl-Phe^r	Fig. 7	This work
LDHhA	UA159 *irvA*::FLAG, *ldh*::HA, Sp^r, Em^s, *p*-Cl-Phe^r	Fig. 7	This work
LDHhAR	UA159 Δ*irvR*, *irvA*::FLAG*, ldh*::HA, Sp^r, Em^s, *p*-Cl-Phe^r	Fig. 7	This work
LDHhAF	UA159 *ldh$_P$*::*irvA*::FLAG, *ldh*::HA, Sp^r, Em^s, *p*-Cl-Phe^r	Fig. 7	This work
WTLFH	UA159::IFDC2, Em^r, *p*-Cl-Phe^s		This work
CALDLFH	UA159::IFDC2, *gyrA$_P$-gbpC*, *irvA* 5' UTR::*gfp*, Em^r, *p*-Cl-Phe^s, Sp^r		This work
CLDLFH	UA159::IFDC2, *gyrA$_P$-gbpC*, *irvA$_P$*::*gfp*, Em^r, *p*-Cl-Phe^s, Sp^r		This work
WTLH	UA159 *ldh*::HA, Em^s, *p*-Cl-Phe^r	Fig. 3	This work
CALDF	UA159 *gyrA$_P$-gbpC*, *irvA* 5' UTR::*gfp*, *ldh*::HA, Sp^r, Em^s, *p*-Cl-Phe^r	Fig. 3	This work
CLDF	UA159 *gyrA$_P$-gbpC*, *irvA$_P$*::*gfp*, *ldh*::HA, Sp^r, Em^s, *p*-Cl-Phe^r	Fig. 3	This work
WTS	UA159 *gbpC*::FLAsH Tag, Em^s, *p*-Cl-Phe^r	Fig. 3	This work
CALDS	UA159 *gyrA$_P$*::*gbpC*, *irvA* 5' UTR::*gfp* *gbpC*::FLAsH Tag, Em^s, *p*-Cl-Phe^r	Fig. 3	This work
CLDS	UA159 *gyrA$_P$*::*gbpC*, *irvA$_P$*::*gfp* *gbpC*::FLAsH Tag, Em^s, *p*-Cl-Phe^r	Fig. 3	This work
SWAP	UA159 *irvA* seed region::*gbpC ORF*, *gbpC* seed region::*irvA* ORF, Em^s, *p*-Cl-Phe^r	Fig. 4	This work
CIRKO	UA159 Δ*gbpC* seed region, Em^s, *p*-Cl-Phe^r	Fig. 4	This work
AIRKO	UA159 Δ*irvA* seed region, Em^s, *p*-Cl-Phe^r	Fig. 4	This work
CRBS1	UA159 *gbpC* RBS mutation, Em^s, *p*-Cl-Phe^r	Fig. S4	This work
CRBS2	UA159 *gbpC* stop codon mutation, Em^s, *p*-Cl-Phe^r	Fig. S4	This work
J2KO	UA159 Δ*rnjB*, Em^r	Fig. 6, S4	This work
YKO	UA159 Δ*rnY*, Km^r	Fig. 6, S4	This work
J1KO	UA159 Δ*rnjA*, Sp^r	Fig. 6, S4	This work
J2KOAKO	UA159Δ*rnjB*, Δ*irvA,*Em^r	Fig. 6, S4	This work
YKOAKO	UA159 Δ*rnY*, Δ*irvA*,Km^r	Fig. 6, S4	This work
J2KOCKO	UA159Δ*rnJB*, Δ*gbpC,* Em^r	Fig. S4	This work
COMJ2	UA159::pDL278J2, Δ*rnjB*, Sp^r, Em^r	Fig. S4	This work
COMY	UA159::pDL278Y, Δ*rnY*, Sp^r, Km^r	Fig. S4	This work
CGFP	UA159 *gbpC*::*gfp*, Em^s, *p*-Cl-Phe^r	Fig. 5	This work
CM1	UA159 *gbpC* point mutations (nt 170 – 173, 188 – 194) , *gbpC*::*gfp*, Em^s, *p*-Cl-	Fig. 5	This work

	Phe^r		
AM1	UA159 *irvA* point mutations (nt 188 – 198), *gbpC*::*gfp*, Em^s, *p*-Cl-Phe^r	Fig. 5	This work
CM2M3	UA159 *gbpC* point mutations (nt 176 – 181, 200 – 203, 206 – 208), *gbpC*::*gfp*, Em^s, *p*-Cl-Phe^r	Fig. 5	This work
AM1CM1	UA159 *gbpC* point mutations (nt 170 – 173, 188 – 194), *irvA* point mutations (nt 188 – 198), *gbpC*::*gfp*, Em^s, *p*-Cl-Phe^r	Fig. 5	This work
GN01RA	UA159 Δ*irvR*, Δ*irvA*, Km^r	Fig. 7	(Niu et al., 2008)
RKOluc	UA159 *irvR$_P$*::*luc*, Δ*irvR*, Km^r	Fig. 7	This work
RKO2luc	UA159 *irvR$_P$*::*luc*, Δ*irvR*, frameshift corrected point mutation in *irvA* ORF, Km^r	Fig. 7	This work
RKO3luc	UA159 *irvR$_P$*::*luc*, Δ*irvR*, stop codon point mutation in the *irvA* ORF, Km^r	Fig. 7	This work
pDL278	*E. coli-Streptococcus* shuttle vector; Sp^r		(Chen and LeBlanc, 1992)
pDL278A	pDL278::*irvA*, Sp^r		This work
pWF5-gfp	pWF5::*ldh$_P$*::*gfp*, Sp^r		This work
pDL278AR	pDL278::*irvA/irvR*, Sp^r		This work
pIFDC2	pDL278::*ldh$_P$*::*mpheS**::*ermAM*, Sp^r, Em^r		(Xie et al., 2011)
pDL278J2	pDL278::RNase J2 Sp^r		This work
pDL278Y	pDL278::RNase Y Sp^r		This work
pDLirvA*	pDL278::*irvA* stop codon point mutation, Sp^r		Unpublished plasmid

Table S1. Strains and plasmids. Related to Figures 1 – 7. Strains and plasmids used in this study are described with their relevant genotypes. The Figure column indicates the manuscript figures utilizing the respective strains. Antibiotic resistances are abbreviated as follows: Em^r, erythromycin resistance; *p*-Cl-Phe^r, 4-chlorophenylalanine resistance; Sp^r, spectinomycin resistance; and Km^r, kanamycin resistance.

Table S2. Primers. A spreadsheet containing all primer sequences has been included as a separate file.

Supplemental Experimental Procedures

Bacterial strains, plasmids, and culture conditions

Escherichia coli cells were grown in Luria-Bertani (LB; Difco) medium at 37 °C. *E. coli* strains carrying plasmids were selected with 100 μg ml^{-1} ampicillin (Fluka) or 150 μg ml^{-1} spectinomycin (Sigma). All *S. mutans* strains were grown anaerobically (85% N_2, 10% CO_2, and 5% H_2) at 37 °C. *S. mutans* strains were cultivated in either brain-heart infusion (BHI) or BTR-G broth (Sato et al., 1997). All cultures grown in the presence of environmental stress were maintained in BTR-G broth supplemented with 0.6% (wt/vol) xylitol. For the selection of antibiotic-resistant colonies, BHI plates were supplemented

with 800 μg ml^{-1} kanamycin (Sigma), 900 μg ml^{-1} spectinomycin (Sigma), 15 μg ml^{-1} erythromycin (MP Biomedicals), or 0.4% DL-4-chlorophenylalanine (Sigma).

DNA manipulation and strain construction

The strains used in this study are described in Table S1. Phusion DNA polymerase, restriction enzymes, T4 DNA ligase and other DNA modifying enzymes were all purchased from New England Biolabs. The PCR primers used in this study are listed in Table S2. The protocol for cloning-independent allelic replacements and markerless mutagenesis of *S. mutans* has been described previously (Xie et al., 2011). The *S. mutans* genome reference strain UA159 is referred to as the wild-type strain throughout this study.

Construction irvA *and* gbpC *deletions for DDAG analysis*

The *gbpC* deletion mutant was generated by allelic replacement. Approximately 1 kb of homologous sequence downstream of the *gbpC* ORF was amplified with the primers gbpCDNF/gbpCDNR, while a similar sized *gbpC* upstream homologous fragment was amplified with the primers irvAF/irvRR. Both PCR amplicons were engineered with complementary sequences to the counter selectable antibiotic resistance cassette IFDC2 cassette. IFDC2 was amplified using the plasmid pIFDC2 (Xie et al., 2011) as a template with the primers IFDF/IFDR. The three PCR amplicons were mixed into a single reaction and assembled using overlap extension PCR with the primers gbpCDNF/irvRR. The resulting amplicon was transformed into UA159 to produce the *gbpC* deletion mutant CKO-IFD2. To create the *irvA* ORF deletion mutant, the *irvA* ORF was replaced in-frame with the *gfp* ORF. First, the *gfp* ORF was amplified using the plasmid pWF5-gfp as a template with the primers GFPF/GFPR, which have complementary sequences to the *aad9* spectinomycin resistance cassette and *irvA* 5' UTR. The *irvA* 5' UTR (with *irvA* ribosome binding site) + *irvA* upstream fragment was amplified with the primers irvALDR/irvRR, which incorporate complementary sequence to the *gfp* ORF. The *gbpC* gene was amplified with the primers gbpCF2/gbpCR, which incorporate complementary sequence to the *aad9* spectinomycin resistance cassette. The spectinomycin resistance cassette was amplified with the primers specF/specR using the plasmid pDL278 as a template. The above PCR fragments were assembled by overlapping PCR with the primers gbpCR/irvRR and subsequently transformed into the wild type UA159 to create the mutant ALDGFP. To construct the complete *irvA* gene deletion mutant (UTR + ORF), two upstream and downstream *irvA* homologous fragments were amplified with the primers irvRF/irvRR and gbpCF/gbpCR, respectively. Both PCR amplicons contain complementary sequences to the counterselectable IFDC2 cassette, which facilitated the ligation of the three amplicons by overlap extension PCR. The resulting PCR amplicon was transformed into UA159 to produce the *irvA* allelic exchange deletion mutant AKO-IFD2. To construct the *irvR* deletion mutant, the *irvR* gene was replaced with the counterselectable IFDC2 cassette using alleleic exchange mutagenesis. Approximately 1 kb of homologous sequence upstream and downstream of *irvR* was amplified with the primers irvRDNF/irvRDNR and irvRUPF/gbpCR. The two amplicons contain complementary sequences, which facilitate their assembly by overlap extension PCR. The resulting amplicon was transformed into AKO-IFD2 to create the *irvR* deletion strain RKO. To generate the *irvA* ORF and *irvR* double mutant, the *irvR* downstream sequence was amplified with the primers irvRDNF2/irvRDNR, which contain complementary sequence to the *irvA* promoter. The *irvA* 5' UTR (with *irvA* promoter) and *gfp* ORF was amplified with the primers irvAF/GFPR2, which contain complementary sequence to the *gbpC* promoter. The *gbpC* gene (with promoter) was amplified with the primers gbpCF3/gbpCR. The three amplicons were ligated using overlap extension PCR with the primers gbpCR/irvRDNR. The resulting amplicon was transformed into strain AKO-IFD2 to generate the *irvA* ORF and *irvR* deletion strain AORFR. For the construction of the complete *irvA* gene (5' UTR + ORF) + *irvR* double deletion mutant, the *irvR* downstream fragment was amplified with the primers

irvRDNF3/irvRDNR, which contain complementary sequence to the *gbpC* promoter. The *gbpC* gene (with promoter) was amplified with the primers gbpCF2/gbpCR. The two amplicons were assembled by overlap extension PCR with the primers gbpCR/irvRDNR. The resulting amplicon was transformed into AKO-IFD2 to generate the complete *irvA* gene + *irvR* deletion strain AKOR.

Construction of gyrA$_P$-gbpC *and truncation variants*

All mutation constructs were assembled using overlap extension PCR and the resulting PCR reactions were transformed directly into *S. mutans* via natural transformation to generate the desired mutant strains. To construct *irvA* and *gbpC* leader deletion mutants in the *gyrA*$_p$-*gbpC* background, we first constructed the *gyrA*$_p$-*gbpC* strain containing an *irvA* 5' UTR-*gfp* fusion. The *gyrA* promoter was amplified with the primers gyrapF and gyrapR, which incorporated sequences complementary to the spectinomycin resistance cassette *aad9* and the 5' region of the *gbpC* gene. The *irvA* locus was amplified with primers irvRR and irvASPEC, which also contain sequences complementary to *aad9*. The *gbpC* gene was amplified with the primers gbpCR and gbpCGF, which have sequences complementary to the *gyrA* promoter and result in a +1 fusion between *gbpC* and the *gyrA* promoter. The spectinomycin resistance cassette was amplified with the primers specF/specR using the plasmid pDL278 as a template. Each of these PCR amplicons were mixed into a single reaction and assembled with overlap extension PCR using the primers gbpCR/irvRR. The resulting PCR reaction was transformed into the wild type *S mutans* UA159 to generate to generate the *gyrA*$_p$-*gbpC* mutant strain GAGBPC. To combine the *irvA* 5' UTR-*gfp* fusion with the *gyrA*$_p$-*gbpC* fusion, we amplified the *irvA* 5' UTR-*gfp* locus from strain ALDGFP using the primers GFPR/irvRR, which have complementary sequences the *aad9* spectinomycin resistance cassette. The *gyrA*$_p$-*gbpC* locus was amplified from GAGBPC using the primers gbpCR/specF. The above PCR fragments were assembled using overlap extension PCR with the primers gbpCR/irvRR and subsequently transformed to wild type UA159 to create the *gyrA*$_p$-*gbpC irvA* 5' UTR-*gfp* fusion strain CALD. To delete the *irvA* 5' UTR from strain CALD, the *gyrA*$_p$-*gbpC* locus was amplified from CALD using the primers gbpCR/GFPF and the truncated *irvA* 5' UTR-*gfp* locus was amplified using the primers irvAPR/irvRR. The irvAPR primer contains complementary sequences to *gfp*, which were used to ligate the two PCR amplicons together using overlap extension PCR and the primers gbpCR/irvRR. The resulting PCR amplicon was transformed into strain UA159 to generate a *gyrA*$_p$-*gbpC* strain containing a truncated *irvA* 5' UTR-*gfp* fusion (strain CLD). To generate the *gbpC* leader deletion mutant strain ALD, the leaderless *gbpC* gene was amplified with the primers gbpCM2F/gbpCR in which gbpCM2F has complimentary sequence to *gyrA* promoter. The upstream fragment containing the *gyrA* promoter *aad9* spectinomycin cassette, and the *irvA* 5' UTR-*gfp* locus was amplified with primers gyrapR/irvRR using CALD gDNA as a template. The two PCR amplicons were mixed and ligated using overlap extension PCR and the primers gbpCR/irvRR. The resulting PCR amplicon was transformed into UA159 to create the strain ALD. To generate the strain CALDKO containing a double deletion of the *irvA* 5' UTR and the *gbpC* 5' UTR, the truncated *irvA* 5' UTR-*gfp* locus was amplified from strain CLD using the primers GFPR/irvRR, while the truncated *gbpC* 5' UTR locus was amplified from strain ALD using the primers specF/gbpCR. The primer GFPR contains complementary sequence to the *aad9* spectinomycin resistance cassette, which allowed the two PCR amplicons to be ligated using overlap extension PCR with the primers gbpCR/irvRR. The resulting PCR amplicon was transformed into UA159 to generate the strain CALDKO.

Construction of epitope tagged ldh *gene for* gbpC *western blot*

A markerless mutagenesis approach was used to add the HA epitope sequence at the 3' of the *ldh* gene. Approximately 1 kb upstream and downstream homologous sequences flanking the *ldh* gene were PCR amplified with the primer pairs ldhUPF/ldhUPR and ldhDNF2/ldhDNR. The primers ldhDNF and ldhUPR contain complementary sequences to the IFDC2 counterselection cassette, which facilitated the subsequent ligation of their respective PCR amplicons with the IFDC2 cassette by

overlap extension PCR. The resulting amplicon was transformed into the wild-type, CALD, and ALD to create the strains WTLFH, CALDLFH, and CLDLFH respectively. Next, the *ldh* gene was PCR amplified with the primers ldh-HF and ldhF, which add a C-terminal HA epitope. Overlap extension PCR was used to ligate this amplicon to 1 kb upstream and downstream homologous sequences generated with the primer pairs ldhUPF/ldhUPR2 and ldhDNF3/ldhDNR. The resulting amplicon was transformed to WTLFH, CALDLFH and ALDLFH to generate the *ldh*-HA fusion strains WTLH, CALDF, and CLDF.

Construction of epitope tagged irvA *and* ldh *genes for IrvA western blot*

A markerless mutagenesis approach was used to construct an epitope tagged *irvA*. To create the IrvA-FLAG fusion, the *irvA* deletion mutant AKO-IFD2 was used as the recipient strain. The *irvA* ORF + upstream homologous region was amplified with the primers irvA-FLAF/irvRR, which also introduce a C-terminal FLAG epitope sequence onto the *irvA* ORF. The region downstream of the *irvA* stop codon was amplified with the primers irvA-FLAR/gbpCR, which contain complementary sequence to the FLAG epitope sequence. These two PCR amplicons were assembled by overlap extension PCR with the primers irvRR/gbpCR and transformed into the strain IFD to create the markerless FLAG-tagged strain AFLA. To construct the *irvR* deletion mutant with a FLAG epitope tagged *irvA, irvR* downstream and upstream fragments were amplified with the primers irvRDNF/irvRDNR and irvRUPF/gbpCR using mutant AFLA genomic DNA as the template. The two amplicons contain complementary sequences that facilitated their ligation via overlap extension PCR. The resulting amplicon was transformed to AKO-IFD2 to generate the mutant strain AFLAR. Next, the HA epitope was added to the C-terminus of the *ldh* gene. The *ldh* gene was amplified with the primers ldh-HF/ldhF, which also incorporate a C-terminal HA epitope sequence. The homologous fragment downstream of the *ldh* stop codon was amplified with the primers ldhDNF/ldhDNR and the spectinomycin resistance gene *aad9* was amplified with specldhF/specR. Complementary sequences in the resulting PCR amplicons facilitated their assembly by overlap extension PCR with the primers ldhF/ldhDNR. The resulting PCR amplicon was transformed into UA159 and AFLA to generate the strains WTLH and ALDHfh respectively. To construct the *ldh-irvA* transcriptional fusion, the *ldh* promoter + native ribosome binding site was amplified with the primers ldhPF/ldhPR. The FLAG-tagged *irvA* + downstream homologous fragment was amplified from strain AFLA with the primers ldhADNF/gbpC R. The upstream fragment flanking the native *irvR* promoter was amplified with the primers ldhAUPF/irvRR. Complementary sequences within the PCR amplicons facilitated their assembly with the primers gbpCR/irvRR. The resulting amplicon containing a +1 fusion of the *ldh* promoter and *irvA* was subsequently transformed into strain IFD to generate the strain ALDH. Next, the HA epitope tagged *ldh* gene locus was amplified with the primers ldhF/ldhDNR from strain WTLH and transformed into ALDH, generating the strain LDHfhF.

Construction of FLAsH epitope tagged GbpC

To construct *gbpC* mutants with an internal FLAsH epitope, the CKO-IFD2 strain was used as a recipient strain to create the three markerless FLAsH tagged *gbpC* strains WTS, CALDS, and CLDS. To create the wild-type FLAsH tagged *gbpC* strain WTS, we amplified a homologous *gbpC* upstream fragment that terminated at codon 240 using the primers gbpCFLAsHF/ irvRR and a homologous *gbpC* downstream fragment starting at codon 241 using the primers gbpCFLAsHR/gbpCDNF. The gbpCFLAsH primers both incorporate the FLAsH epitope nucleotide sequence, which allows the assembly of the two PCR amplicons by overlap extension PCR using the primers gbpCDNF/irvRR. The resulting PCR amplicon was transformed to CKO-IFD2 to produce WTS. To create the FLAsH tagged *gbpC* in the $gyrA_P$-*gbpC* background, we amplified the $gyrA_P$-*gbpC* fusion up to codon 240 using the primers gbpC-FLAsHF/gyrapF, along with the *gbpC* downstream fragment starting at codon 241 amplified with gbpC-FLAsHR/gbpCDNF, and the *irvA* 5' UTR-*gfp* locus amplified with irvAR2/irvRR. Complementary sequences in the three amplicons facilitated their subsequent ligation

by overlap extension PCR using the primers gbpcDNF/irvRR. The resulting PCR amplicon was transformed into CKO-IFD2 to create CALDS. To create the FLAsH tagged *gbpC* in the *gyrA*$_P$-*gbpC* strain containing a truncated *irvA* 5' UTR, we used the same strategy except that the truncated *irvA* 5' UTR-*gfp* locus was amplified from the strain CLD. The resulting overlap extension PCR amplicon was transformed into strain CKO-IFD to create the strain CLDS.

Construction of gbpC *translation deficient mutants*

To mutate the *gbpC* ribosome binding site, point mutations were introduced into the primer gbpCM1F. The *gbpC* upstream homologous region was amplified with the primers gbpCM1F/irvRR. A fragment encompassing the *gbpC* ORF and downstream homologous region was amplified with the primers gbpCM1R/gbpCDNF. The gbpCM1R primer included complementary sequence to gbpCM1F. The two PCR amplicons were ligated by overlap extension PCR using the primers gbpCDNF/irvRR. The resulting PCR amplicon was transformed into CKO-IFD2 to create the strain CRBS1. To delete the *irvA* gene from CRBS1, we amplified the *gbpC* ribosome binding site mutant *gbpC* locus from strain CRBS1 using the primers gbpCDNF/gbpCF3 and we amplified the truncated *irvA* 5' UTR-*gfp* fusion locus from strain CLD using the primers GFPR2/irvRR. Complementary sequences between the two amplicons facilitated their ligation using overlap extension PCR with the primers gbpCDNF/irvRR. The resulting PCR amplicon was transformed to CKO-IFD2 to create the strain RBS1A. To introduce a stop codon immediately after the *gbpC* translation start codon, a TAG stop codon was introduced into the primer gbpCM3F. The *gbpC* upstream region was amplified with gbpCM3F/irvRR, while the *gbpC* ORF + downstream homologous fragment was amplified with the primer gbpCM3R/gbpCDNF. Complementary sequences between the two amplicons facilitated their ligation using overlap extension PCR with the primers gbpCDNF/irvRR. The resulting PCR amplicon was transformed into CKO-IFD2 to create the strain CRBS2. To delete the *irvA* gene from CRBS2, we amplified the *gbpC* stop codon mutant *gbpC* locus from strain CRBS2 using the primers gbpCDNF/gbpCF3 and we amplified the truncated *irvA* 5' UTR-*gfp* fusion locus from strain CLD using the primers GFPR2/irvRR. Complementary sequences between the two amplicons facilitated their ligation using overlap extension PCR with the primers gbpCDNF/irvRR. The resulting PCR amplicon was transformed to CKO-IFD2 to create the strain RBS2A.

Construction of RNase J1, J2, and Y mutants

To generate deletions of RNases J1, J2, and Y, two homologous fragments corresponding to approximately 1 kb upstream and downstream of each ORF was generated by PCR with the primer pairs J1UPF/J1UPR and J1DNF/J1DNR (RNase J1), J2UPF/J2UPR and J2DNF/J2DNR (RNase J2), and YUPF/YUPR and YDNF/YDNR (RNase Y). Each of the primer sets incorporated sequences complementary to either the spectinomycin resistance cassette *aad9* (RNase J1), the kanamycin resistance cassette (RNase Y) or the erythromycin resistance cassette *ermAM* (RNase J2). The erythromycin resistance cassette was amplified using primers ermF/ermR, while the spectinomycin resistance cassette was amplified using the primers specF/specR. The corresponding PCR amplicons for all three constructs were ligated by overlap extension PCR. The resulting PCR amplicons were transformed into UA159 to generate allelic replacement mutant strains of RNase J1 (J1KO), RNase J2 (J2KO), and RNase Y (YKO). The same RNase J2 and RNase Y mutagenesis constructs were also transformed into strain AKO to produce the double mutant strains J2KOAKO and YKOAKO. Additionally, the RNase J2 mutagenesis construct was transformed into strain CKO to produce the double mutant J2KOCKO.

Site-directed mutagenesis of gbpC *and* irvA *seed pairing regions*

To validate the seed pairing between *gbpC* and *irvA* mRNA, we employed a strategy to monitor *gbpC* mRNA stability *in situ* based upon GFP fluorescence. First we created a markerless operon fusion between the *gbpC* and *gfp* ORFs. The *gfp* ORF + ribosome binding site was amplified with the primers GFPFF/GFPR2. Approximately 1 kb *gbpC* downstream homologous fragment was amplified

with gbpCDNF/gbpCDNR3, while the *gbpC* gene and its upstream was amplified with primers CUPF/irvRR. Both homologous fragments contain complementary sequences with *gfp*, which facilitated their ligation by overlap extension PCR. The resulting amplicon was transformed to CKO-IFD2 to produce the *gbpC-gfp* operon fusion strain CGFP. To mutate predicted seed pairing bases in *gbpC*, the desired point mutations were incorporated into the primer cm1F. Next, the downstream homologous fragment of the *gbpC-gfp* operon fusion was amplified from strain CGFP using the primers cm1F/gbpCDNF. The *gbpC* upstream homologous fragment was amplified with the primers cm1R/irvRR. Complementary sequence between the two PCR amplicons facilitated their ligation by overlap extension PCR. The resulting amplicon was transformed into CKO-IFD2 to generate the *gbpC* point mutant strain CM1. As a negative control, we also introduced two separate series of *gbpC* point mutations at predicted unpaired bases of *gbpC*. The *gbpC* gene fragment containing first series of point mutations + upstream homologous region was obtained by PCR with the primers cm2R/irvRR. The mutated bases were incorporated into the primer cm2R. The *gbpC* gene fragment containing the second series of point mutations was amplified with the primers cm2F/cm3R. The primer cm2F has complementary sequence to cm2R, while the desired point mutations were incorporated into the primer cm3R. The *gbpC* downstream homologous fragment was amplified with the primers cm3F/gbpCDNF. The primer cm3F has complementary sequence to cm3R. The three amplicons were mixed and used as template for overlap extension PCR with primers gbpCDNF/irvRR. The resulting amplicon was transformed to CKO-IFD2 to generate *gbpC* interaction region point mutant CM2M3. Next, a portion of the *irvA* 5' UTR and *irvA* upstream region was amplified with primers Am1F/irvRR, which introduced the desired mutant bases into the *irvA* 5' UTR. The remaining portion of *irvA* and the *irvA* downstream region was amplified with the primers Am1R/gbpCDNF using CGFP genomic DNA as a template. Complementary sequences between the two fragments facilitated their assembly by overlap extension PCR. The resulting amplicon was transformed into AKO-IFD2 to create the *irvA* point mutant strain AM1. To create the compensating mutations in the seed pairing bases of *gbpC* and *irvA*, the *gbpC* upstream homologous fragment containing the *irvA* point mutations was amplified with the primers cm1R/irvRR from the strain AM1. The downstream homologous fragment containing the *gbpC-gfp* operon fusion was amplified from strain CGFP using the primers cm1F/gbpCDNF, which introduce the *gbpC* point mutations. Complementary sequence between the two PCR amplicons facilitated their ligation by overlap extension PCR. The resulting amplicon was transformed into CKO-IFD2 to generate the strain AM1CM1 containing two sets of compensatory seed pairing mutations.

Construction of mRNA interaction domain mutants for RACE walk analysis

To construct the *irvA* interaction region deletion mutant, the *irvA* promoter and upstream homologous region was amplified with the primers irvAIRF/irvRR. The *irvA* ribosome binding site + ORF and downstream homologous region was amplified with the primers irvAIRR/gbpCR. Complementary sequence between the two PCR amplicons facilitated their assembled by overlap extension PCR. The resulting PCR amplicon was transformed to AKO-IFD2 to generate the mutant strain AIRKO. To construct the *gbpC* interaction region deletion mutant, two *gbpC* homologous fragments were generated by PCR with the primer pairs gbpCIRF/irvRR and gbpCIRR/gbpCDNF. Complementary sequence between the two PCR amplicons facilitated their assembly by overlap extension PCR. The resulting PCR amplicon was transformed into CKO-IFD2 to generate the mutant strain CIRKO. To create the *gbpC* and *irvA* interaction region swap mutant, we first produced two overlap extension PCR amplicons containing the respective domain swaps of *gbpC* and *irvA*. These two constructs were subsequently used in a final overlap extension PCR reaction to ligate the two constructs together. For the replacement of the *irvA* interaction region, the *gbpC* interaction region was amplified with the primers gbpCSWAPF/gbpCSWAPR, which contain complementary sequence to *irvA* upstream homologous region. The *irvA* ORF and *gbpC* promoter region was amplified with the

primers irvALDSR/gbpCLDSR, which contain complimentary sequence to the *gbpC* and *irvA* interaction region. The *irvA* upstream homologous region was amplified with the primers irvRF2/irvRR, which contain complementary sequences to the *gbpC* interaction region. The three PCR amplicons were assembled by overlap extension PCR using the primers gbpCLDSR/irvRR to create the resulting amplicon CSWAP-R. For the replacement of the *gbpC* interaction region, the *irvA* interaction region was amplified with the primers irvASWAPF/irvASWAPR. The *gbpC* ORF and downstream region were amplified with the primers gbpCDNF/gbpCDNR2, which contain complementary sequences to the *irvA* interaction region. These two PCR products were assembled by overlap extension PCR with the primers irvASWAPF/gbpCDNR to create the resulting amplicon ASWAP-CDN. The two amplicons CSWAP-R and ASWAP-CDN contained complementary sequence, which facilitated their assembly by a final overlap extension PCR reaction. The resulting amplicon was transformed to strain CKO-IFD2 to generate the mutant strain SWAP. To generate the *irvA* 5' UTR internal deletion strain used in Figure 4, the primer pairs STD3F/gbpCR and STD3R/irvRR were used to amplify the downstream and upstream regions surrounding the deletion site using genomic DNA extracted from strain CALD. The resulting PCR amplicons were assembled by overlap extension PCR with the primers gbpCR/irvRR and transformed into the wild-type UA159 to generate the mutant strain ASTD3.

Construction of irvA*,* irvA/irvR, *RNase J2, and RNase Y complementation vectors*

The *irvA*, *irvA/irvR*, *rnjB,* and *rny* genes were amplified with the primers AcomF/AcomR, ARcomF/AcomR, J2comF/J2comR, and YcomF/YcomR, respectively using Phusion DNA polymerase (NEB). Each primer pair incorporated EcoR1 and BamH1 restriction sites. The resulting PCR amplicons were digested with EcoR1 and BamH1 (NEB) and ligated to compatible sites on the *E. coli-Streptococcus* shuttle vector pDL278. The resulting plasmids were sequenced and the confirmed constructs were transformed into strains AKO-IFD2, AKOR, J2KO, and YKO, respectively to generate the complementation mutants COMA (*irvA*), COMAR (*irvR/irvA*), COMJ2 (*rnjB*), and COMY (*rny*).

Construction of strains for IrvA competence assay

Four strains were compared for their natural competence ability. The Δ*irvR/A* double mutant strain GN01RA were created by allelic replacement and has been previously described (Niu et al., 2008). The following three mutant strains were created using a similar strategy to replace the *irvR* ORF with a firefly luciferase ORF, which was used to examine the expression of the *irvR* promoter in an unrelated experiment. The allelic replacement of *irvR* was created as follows. The *irvR* upstream homologous fragment containing the *irvR* promoter was amplified with the primers gbpCR/ARlucUpR, which incorporated complementary sequence to the luciferase cassette. The firefly luciferase cassette was amplified with the primers luciF/luciR, which incorporated complementary sequence to the *aphAIII* kanamycin resistance cassette. The *irvR* downstream homologous fragment was amplified using the primers KanF/irvRR using the previously constructed kanamycin resistant Δ*irvR* allelic replacement mutant strain GN01R (Niu et al., 2008) as a template. The amplicons were assembled using overlap extension PCR and the primers gbpCR/irvRR. The resulting amplicon was transformed into the wild-type UA159 to create the firefly luciferase ORF allelic replacement of the *irvR* ORF (strain RKOluc). To create the *irvR* deletion mutant expressing a frameshift corrected *irvA*, we amplified the *irvR* upstream homologous fragment from the wild-type strain UA140 using the primers gbpCR/ARlucUpR, which incorporated complementary sequence to the luciferase cassette. The luciferase cassette and *irvR* downstream homologous region was amplified from strain RKOluc using the primers luciF/irvRDNR. The two PCR amplicons were assembled using overlap extension PCR with the primers gbpCR/irvRDNR and transformed into UA159 to generate the strain RKO2luc. To create the *irvR* deletion mutant expressing *irvA* with a premature stop codon, *gbpC* was amplified with the primers gbpCF3/gbpCR, the *irvA* gene containing a stop codon was amplified from the plasmid pDLirvA* (unpublished plasmid) using the primers irvARG/ARlucUpR, and the *irvR* downstream homologous region was amplified from strain RKOluc using the primers luciRDNF/irvRDNR.

Complementary sequences in the amplicons facilitated their assembly using overlap extension PCR with the primers gbpCR/irvRDNR. The resulting amplicon was transformed into UA159 to create the strain RKO3luc.

Total RNA extraction

Overnight cultures of *S. mutans* were diluted 1:40 in fresh BTR-G medium +/- 0.6% (wt/vol) xylitol and grown at 37 °C to mid-log phase. RNA extraction was performed as previously described (Niu et al., 2008). RNA pellets were dissolved in DEPC-treated water and stored at -80 °C.

Northern blot analysis

RNA samples were frozen and thawed no more than once to minimize degradation. Total RNA was separated on a 1% agarose 0.66 M formaldehyde gel in a buffer consisting of 40 mM 3-(N-morpholino)propanesulfonic acid (MOPS) (pH 7.0), 10 mM sodium acetate, and 0.2 mM EDTA. RNA was then transferred to a Hybond-N membrane (Amersham) in a Trans-Blot SD Semi-Dry Transfer Cell (Bio-Rad) and immobilized to the membrane by UV crosslinking (Stratagene). Gene-specific digoxigenin (DIG) probes were either PCR-generated using a PCR DIG probe synthesis kit (Roche Diagnostic) or synthesized via *in vitro* transcription using DIG-UTP (Roche) according to the manufacturer's instructions. Primers used for DIG probe synthesis are listed in Supplemental Materials. Hybridization of the DIG-labeled probes and visualization with CDP-Star were performed according to the manufacturer's instructions. The abundance of 16S rRNA was visualized by ethidium bromide staining and served as a loading control.

Preparation of protein samples

S. mutans cells were grown overnight at 37 °C in 1 ml of BHI medium. The overnight cultures were diluted 1:30 in BTR-G or BTR-G plus 0.6% xylitol in a total volume of 30 ml. The cells were grown to mid log phase and collected by centrifugation. Extraction of total protein was performed using a previously described protocol (Niu et al., 2010). For GbpC protein detection, cells received an additional treatment with 500 U μl^{-1} mutanolysin at 37 °C for 2 hr prior to mechanical disruption to release cell wall proteins. C-terminal His-tagged RNase J2 was overexpressed using pET29b in *E. coli* BL21(DE3) pLysS cells and purified on Cobalt Talon affinity resin (Clontech) similarly as previously described (Condon et al., 2008)

Random mutagenesis of *irvA* by error-prone PCR

For mutagenesis experiments, 100 pg template *irvA* gene was amplified using 0.5 μl of GoTaq® DNA polymerase (5 U μl^{-1}, Promega) in a 20 μl reaction containing the primers AEPF/AEPR at 0.5 μM, 7 mM MgCl2, 10 mM Tris-HCl (pH 8.3), 50 mM KCl, 500 μM dATP, dCTP, dGTP, TTP, dPTP (Trilink Biotech) and 8-oxodGTP (Sigma). After 30 PCR cycles (92°C for one minute, 55°C for 1.5 minute, 72°C for 5 minutes), 1 μl of the amplified material was used in second PCR in which the above conditions were used except that no dPTP or 8-oxodGTP was added to the reaction mixture. The product of the second PCR reaction was mixed with PCR amplicons of *irvA* upstream and downstream fragments amplified with the primers APR/irvRR and AORFF/gbpCDNF, respectively. The reaction mixture was assembled using overlap extension PCR and transformed into the recipient strain AKO-IFD2 to generate a library of 80,000 mutant *irvA* clones.

Determination of *irvA* nucleotides required for DDAG

Approximately 80,000 *S. mutans* colonies harboring randomly mutagenized *irvA* genes were mixed, briefly sonicated to disperse the cells, and diluted into 20 ml cultures of BTR-G medium containing 0.6% xylitol to a final OD_{600} of 0.5. The cultures were incubated for an additional 6 hr before adding

dextran to a final concentration of 100 μg ml^{-1}. DDAG^{+} aggregated cells were pelleted by low speed centrifugation at 700 x g for 1 min., whereas DDAG^{-} mutants remained suspended in the medium. The non-aggregated DDAG^{-} fraction of cells was presumed to contain mutations in critical seed pairing nucleotides of *irvA*. Genomic DNA was extracted from the DDAG^{-} fraction of each culture and used as templates for PCR amplification of *irvA*. The PCR products were quantified using a Qubit dsDNA HS Assay kit (Invitrogen) and equimolar concentrations of each reaction were combined into a single mixture that was subsequently sequenced with an Illumina MiSeq next generation sequencer. Biostatistical analysis using the chi-square test was performed to compare the ratio of mutant sequence to wild-type at each position in the sequence data alignments to determine which nucleotides in *irvA* were significantly enriched for mutations. Nucleotides with significant increases in mutation frequency (p<0.05) were selected as candidate seed pairing nucleotides, while those with insignificant changes (p>0.05) were considered as unpaired nucleotides and used as negative controls in the subsequent validation experiments. A variety of predicted seed pairing and unpaired nucleotides in *irvA* were mutagenized and tested for their effect upon the DDAG response. The experiment was repeated to assess reproducibility.

First strand cDNA synthesis

RNA obtained from affinity purification was treated with 5U DNase I (Ambion) at 37 °C for 30 min. and then purified using the RNeasy MinElute cleanup kit (Qiagen). 500 ng RNA was mixed with 1 μl (100mM) dNTP mix (Promega) and 0.6 μl 50 μM random hexamer (Invitrogen). The mixture was incubated at 65 °C for 10 min. and then chilled on ice. AffinityScript MT reverse transcriptase (Agilent) was used for cDNA synthesis. Each 25 μl reaction contained 1 μl reverse transcriptase, 2.5 μl 10x enzyme buffer, 2 μl (100 mM) DTT, and 0.5 μl RNaseOut ribonuclease inhibitor. The reaction was incubated at 42 °C for 1 hr.

Supplemental References

Ajdic, D., McShan, W.M., McLaughlin, R.E., Savic, G., Chang, J., Carson, M.B., Primeaux, C., Tian, R., Kenton, S., Jia, H.*, et al.* (2002). Genome sequence of Streptococcus mutans UA159, a cariogenic dental pathogen. Proceedings of the National Academy of Sciences of the United States of America *99*, 14434-14439.

Biswas, I., Drake, L., and Biswas, S. (2007). Regulation of gbpC expression in Streptococcus mutans. Journal of bacteriology *189*, 6521-6531.

Chen, Y.Y., and LeBlanc, D.J. (1992). Genetic analysis of scrA and scrB from Streptococcus sobrinus 6715. Infection and immunity *60*, 3739-3746.

Condon, C., Pellegrini, O., Mathy, N., Benard, L., Redko, Y., Oussenko, I.A., Deikus, G., and Bechhofer, D.H. (2008). Assay of Bacillus subtilis ribonucleases in vitro. Methods in enzymology *447*, 277-308.

Niu, G., Okinaga, T., Qi, F., and Merritt, J. (2010). The Streptococcus mutans IrvR repressor is a CI-like regulator that functions through autocleavage and Clp-dependent proteolysis. Journal of bacteriology *192*, 1586-1595.

Niu, G., Okinaga, T., Zhu, L., Banas, J., Qi, F., and Merritt, J. (2008). Characterization of irvR, a novel regulator of the irvA-dependent pathway required for genetic competence and dextran-dependent aggregation in Streptococcus mutans. Journal of bacteriology *190*, 7268-7274.

Sato, Y., Yamamoto, Y., and Kizaki, H. (1997). Cloning and sequence analysis of the gbpC gene encoding a novel glucan-binding protein of Streptococcus mutans. Infection and immunity *65*, 668-675.

Xie, Z., Okinaga, T., Qi, F., Zhang, Z., and Merritt, J. (2011). Cloning-independent and counterselectable markerless mutagenesis system in Streptococcus mutans. Applied and environmental microbiology *77*, 8025-8033.